PHYSICAL REVIEW C VOLUME 51, NUMBER 3 MARCH 1995

Quantal particle flux and nuclear halo effects

R. da Silveira and S. Klarsfeld
Division de Physique Théorique, Institut de Physique Nucléaire, 91406 Orsay Cedex, France

A. Boukour and Ch. Leclercq-Willain
Physique Nucléaire Théorique et Physique Mathématique, Université Libre de Bruxelles, 1050 Bruxelles, Belgium
(Received 20 October 1994)

We propose a method to study refractive scattering by looking at the quantal particle flux within the volume occupied by the nuclear potential. The method is applied to discuss nuclear halo effects in the elastic scattering of ^{11}Li and ^{11}C on ^{12}C at $E/A \sim 60$ MeV.

PACS number(s): 25.70.Bc, 24.10.Ht

The recently measured angular distributions of ^{11}Li+^{12}C and ^{11}C+^{12}C scattering at $E/A \sim 60$ MeV [1] reveal for both systems a characteristic pattern of surface refractive scattering: the ratio σ/σ_R exhibits an (Airy-like) bump beyond which it decreases almost exponentially. Moreover, for ^{11}Li+^{12}C the ratio σ/σ_R was found to be much larger than for ^{11}C+^{12}C. This was considered as providing evidence for additional refractive effects due to the existence of a "halo" in the exotic ^{11}Li nucleus [2]. Soon after, it was pointed out [3,4] that such an interpretation is perhaps not quite so clear, simply because the Rutherford cross section itself is already responsible to a large extent for this effect (for ^{11}Li σ_R is 4 times smaller than for ^{11}C). So the question remains of how to compare the amount of refractive scattering in these two systems. In the present Brief Report we try to do this by looking at the quantal particle flux [5] in two important regions: (i) at large distances, by evaluating the scattering cross section $d\sigma/d\Omega = |f(\theta)|^2$ which is proportional to the magnitude of the scattered flux; (ii) at small distances, $r \sim R_1 + R_2$, where refraction takes place, by calculating the particle flux from the scattering wave function obtained by fitting the data via $|f(\theta)|^2$.

To begin with let us write the wave function for the relative motion in the form

$$\psi(\mathbf{r}) = A(\mathbf{r}) \exp[i\phi(\mathbf{r})], \tag{1}$$

where $A(\mathbf{r})$ and $\phi(\mathbf{r})$ are real. The particle flux per unit time at point $\mathbf{r}$ is given by

$$\mathbf{S}(\mathbf{r}) = (\hbar/m) A^2(\mathbf{r})\, \mathrm{grad}\, \phi(\mathbf{r})\,. \tag{2}$$

Further, we shall assume that the incident energy is large compared with the interaction potential and use Glauber's high-energy approximation [6] to write $\psi(\mathbf{r})$ in the form

$$\psi(\mathbf{r}) = \exp\left\{ ik \left[z - \frac{1}{2E} \int_{-\infty}^{z} V(r)\, dz \right] \right\}, \tag{3}$$

where we have chosen the positive z axis along the direction of propagation $\mathbf{k}$. In (3), $V(r)$ is the nuclear complex optical potential plus a Coulomb term:

$$V(r) = V_{\mathrm{Coul}}(r) + U(r) + iW(r)\,. \tag{4}$$

It is interesting to notice that the approximation (3) is valid mainly in the volume occupied by the potential. This is precisely what we need for evaluating both the scattering amplitude and the particle flux in the surface region. Taking into account the special symmetry of the problem it is convenient to use cylindrical coordinates and to project vectors on the incident direction $\mathbf{k}$ and on the perpendicular plane. Thus

$$\mathbf{r} = \mathbf{b} + z\hat{\mathbf{k}}\,, \quad \mathbf{S} = S_b \mathbf{b}/b + S_z \hat{\mathbf{k}}\,, \tag{5}$$

where b is the usual impact parameter and $\hat{\mathbf{k}} = \mathbf{k}/k$ is the unit vector on the z axis.

The magnitude of the incident flux is obviously $S_i = \hbar k/m = v$, where v is the relative velocity of the two nuclei. One easily obtains $[r = (b^2 + z^2)^{1/2}]$

$$\frac{S_b}{S_i} = -A^2(\mathbf{r}) \frac{1}{2E} \int_{-\infty}^{z} \frac{d}{db} [U(r) + V_{\mathrm{Coul}}(r)]\, dz \tag{6}$$

and

$$\frac{S_z}{S_i} = A^2(\mathbf{r}) \left\{ 1 - \frac{1}{2E} [U(r) + V_{\mathrm{Coul}}(r)] \right\}, \tag{7}$$

where

$$A^2(\mathbf{r}) = \exp\left[\frac{k}{E} \int_{-\infty}^{z} W(r)\, dz \right]. \tag{8}$$

At high energies, apart from the attenuation factor $A^2(\mathbf{r})$, the longitudinal component S_z remains almost unaffected by the real part of the interaction potential. The interesting information about refraction therefore comes from the transversal component S_b. Indeed, the latter measures the departure of the flux vector from the incident direction $\mathbf{k}$. Let us now consider the asymptotic region. Here the magnitude of the outgoing radial scattered flux S_r is given by

$$\frac{S_r}{S_i} = |f(\theta)|^2/r^2 \quad (r \gg R_1 + R_2)\,. \tag{9}$$

So the experimentally determined differential cross section $|f(\theta)|^2$ is nothing but a measure of the outward scattered flux at large distances from the target. Using (3) one obtains the well-known formula

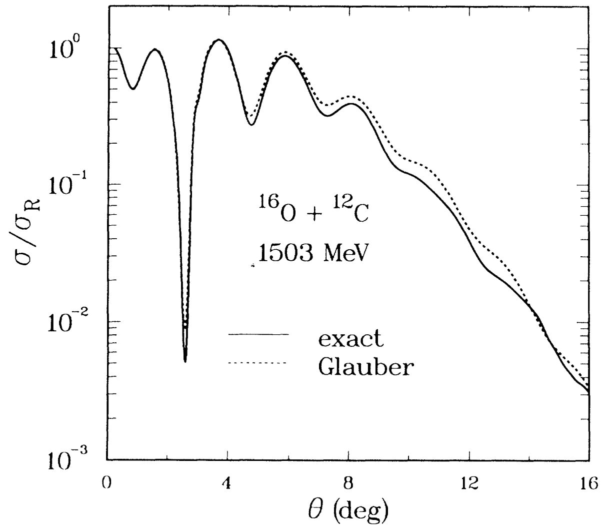

FIG. 1. Calculated elastic scattering angular distribution of $^{16}O+^{12}C$ at 1503 MeV (solid line = exact, dotted line = Glauber approximation). The optical potential parameters are given in (11) (see text).

$$f(\theta) = -ik \int_0^\infty b\,db \left\{ \exp\left[-i\frac{k}{2E}\int_{-\infty}^{\infty} V(r)\,dz \right] - 1 \right\} J_0(qb)\,, \quad q = 2k\sin\theta/2\,, \tag{10}$$

where J_0 denotes a Bessel function [6].

In order to get some familiarity with the use of the particle flux we shall first test its ability to clarify the semiclassical picture according to which the bump in the ratio σ/σ_R is a signature of refractive scattering. To this end we consider the neighboring system $^{16}O+^{12}C$ at $E/A \sim 100$ MeV. The reason for this choice is twofold. (i) An extensive optical model analysis of the data indicates the importance of refractive effects in this system [7]. (ii) The scattering data are purely elastic, contrary to what happens for $^{11}Li+^{12}C$ and $^{11}C+^{12}C$ which include contributions from inelastic scattering with excitation of low-lying states.

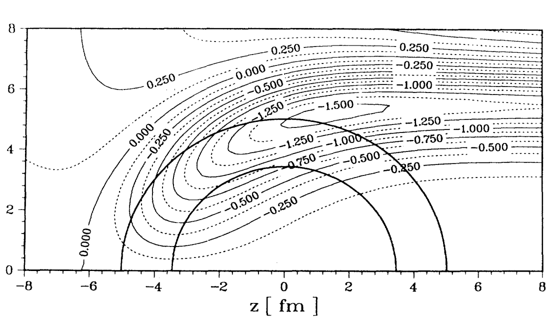

FIG. 2. Contour map of the ratio $\frac{S_b}{S_i}$ ($\times 10^2$) in the (b,z) plane for $^{16}O+^{12}C$ elastic scattering at 1503 MeV. Same optical potential as in Fig. 1. The two semicircles of radii $R \pm a_U$ delimit approximately the surface region.

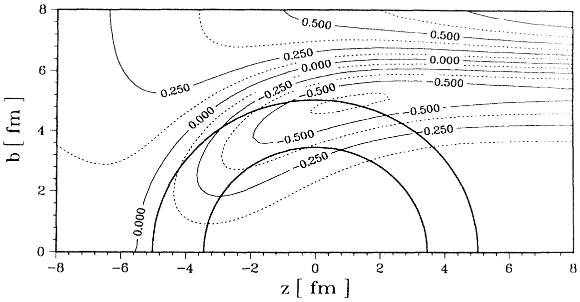

FIG. 3. Same as Fig. 2 except that $U_0 = 40$ MeV while the other parameters are fixed at their values (11).

In our present analysis of the ^{16}O data we used the Woods-Saxon potential of Ref. [7] ($\chi^2 = 1.07$) with parameters

$$\begin{aligned} U_0 &= 80 \text{ MeV}\,, \quad r_U = 0.881 \text{ fm}\,, \\ a_U &= 0.784 \text{ fm}\,, \quad W_0 = 28.8 \text{ MeV}\,, \\ r_W &= 1.008 \text{ fm}\,, \quad a_W = 0.8 \text{ fm}\,. \end{aligned} \tag{11}$$

In Fig. 1 we have plotted the ratio σ/σ_R (dotted curve) calculated from Eq. (10) (for the experimental data see Ref. [7]). The solid line is the result of an "exact" calculation, done by solving numerically the Schrödinger equation to get the phase shifts and by then summing up the partial wave series for the scattering amplitude. It is apparent that the high-energy approximation reproduces quite well the exact result over most of the angular range of interest. Fig. 2 shows a contour map of the ratio $\frac{S_b}{S_i}$ in the (b,z) plane calculated using Eq. (6) with the optical potential (11). The two semicircles with radii $R \pm a_U$ delimit approximately the surface region. This contour map presents some interesting features: (i) On the illuminated face of the target, S_b is negative due to the strong attractive nuclear force. As a result, the vector **S** in Eq. (5) points through "negative" angles as expected from classical arguments. (ii) On the dark face of the target, S_b is negligible. This is a manifestation of the shadow effect due to absorption. (iii) As regards the magnitude of S_b the map exhibits a mountain surrounding the target core, with a crest near the edge.

To test the ability of the particle flux to measure surface scattering let us consider the result of a simulated change in the nuclear refraction on the contour map of S_b. To this end we have varied the strength parameter U_0

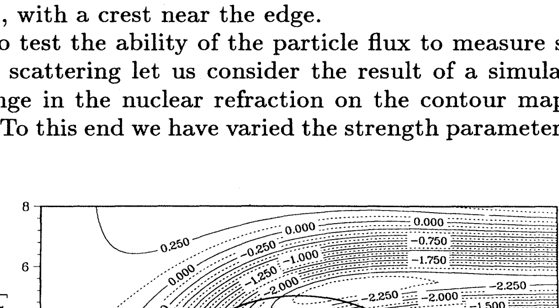

FIG. 4. Same as Fig. 2 except that $U_0 = 120$ MeV.

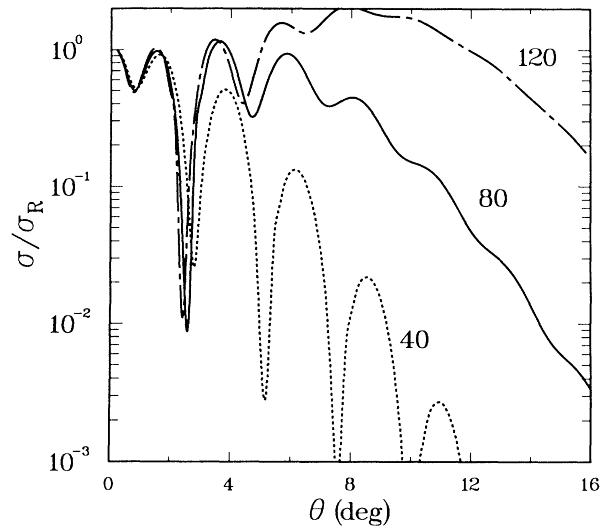

FIG. 5. Calculated elastic angular distributions of $^{16}O+^{12}C$ at 1503 MeV for three different values of U_0 (see text).

while keeping the other parameters of the potential fixed at their values (11). Figures 3 and 4 show the contour maps of S_b obtained by setting, respectively, $U_0 = 40$ and 120 MeV. Comparison with the map in Fig. 2 shows indeed that the particle flux reflects well the changes in the refractive component of the potential. One can also check the semiclassical statement that the bump in the ratio σ/σ_R is due to surface refraction by calculating the angular distributions for the same modified values of U_0. The results are shown in Fig. 5. It is seen that when the surface flux increases ($U_0 = 120$ MeV) the bump in the ratio σ/σ_R is strongly enhanced. In contrast, when the surface flux diminishes ($U_0 = 40$ MeV) the bump almost disappears and the angular distribution presents a diffractionlike pattern.

We now apply the same analysis to study surface scattering in the case of ^{11}Li (^{11}C) + ^{12}C. To this end we use the optical potentials given in Ref. [2]. These potentials have been obtained by generating an elastic cross section which is added to the inelastic cross section given by a distorted-wave Born approximation (DWBA). The potential parameters were then adjusted to optimize the

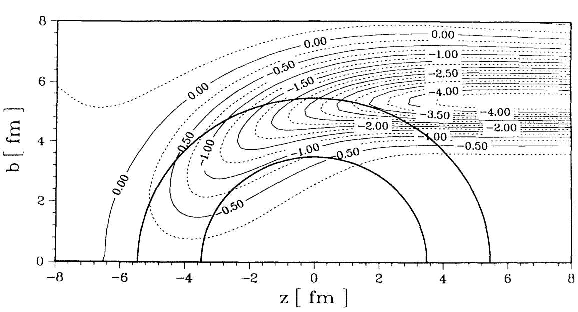

FIG. 6. Contour map of the ratio $\frac{S_b}{S_i}$ ($\times 10^2$) for $^{11}C+^{12}C$ elastic scattering at 620 MeV. Optical model parameters from Ref. [2].

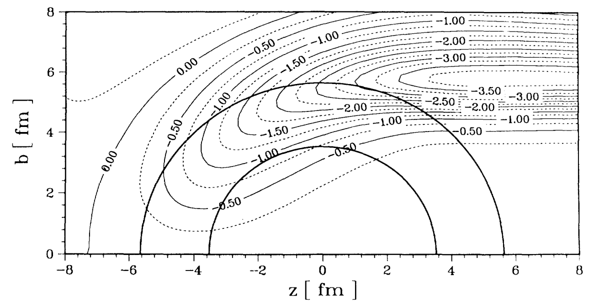

FIG. 7. Contour map of the ratio $\frac{S_b}{S_i}$ ($\times 10^2$) for $^{11}Li+^{12}C$ elastic scattering at 637 MeV. Optical model parameters from Ref. [2].

fit of the total cross section to the measured data. For $^{11}C+^{12}C$ the potential has a Woods-Saxon shape. In turn, for $^{11}Li+^{12}C$, Mermaz [2] found it necessary to add to the usual complex Woods-Saxon potential a complex surface term peaked very far outside the nucleus core. The latter was taken as a derivative of a Woods-Saxon shape. Figures 6 and 7 show the contour maps of $\frac{S_b}{S_i}$ for ^{11}C and ^{11}Li projectiles, respectively, obtained with the Mermaz potentials.

A striking feature of Figs. 6 and 7 is that the two maps are quite similar, in spite of the additional surface term introduced in the potential for ^{11}Li. This simply means that ^{11}Li scattering is not more refractive than ^{11}C scattering. In other words, we claim that there is no evidence so far for a nuclear halo effect in the $^{11}Li+^{12}C$ system. Furthermore, since the surface flux is almost the same for both ^{11}C and ^{11}Li, their angular distributions should also be very similar outside the near-forward direction. In order to make a meaningful comparison of these angular distributions we proceed as in Ref. [4] on dividing

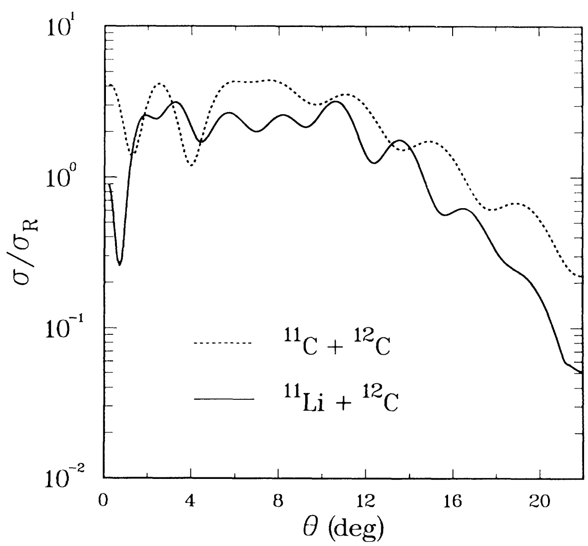

FIG. 8. Calculated angular distributions of ^{11}Li and ^{11}C elastic scattering on ^{12}C. Both differential cross sections are divided by that for Rutherford scattering of ^{11}Li. Optical model parameters from Ref. [2].

them both by the same Rutherford cross section, say, the one for ^{11}Li . The results are plotted in Fig. 8 where one remarks that the ratio for ^{11}C takes the value 4 at zero angle (the charge of ^{11}C is twice that of ^{11}Li). Inspection of these curves confirms the conclusions drawn from the analysis of the surface flux maps. The enhancement in the ratio σ/σ_R, which according to semiclassical arguments is a measure of refractive scattering, is roughly the same for the two projectiles in the angular range contributing most to the total elastic scattering cross section.

To summarize, we have proposed a direct method to analyze refractive scattering by calculating the quantal particle flux within the volume occupied by the nuclear potential. The present approach should be considered as complementary to the conventional one in which the refractive contribution to the angular distribution is identified by semiclassical arguments.

The Division de Physique Théorique is Unité de Recherche des Universités Paris 6 et Paris 11 associée au CNRS.

[1] J. J. Kolata, M. Zahar, R. Smith, K. Lamkin, M. Belbot, R. Tighe, B. M. Sherrill, N. A. Orr, J. S. Winfield, J. A. Winger, S. J. Yennello, G. R. Satchler, and A. H. Wuosmaa, Phys. Rev. Lett. **69**, 2631 (1992).
[2] M. C. Mermaz, Phys. Rev. C **47**, 2213 (1993).
[3] R. da Silveira, S. Klarsfeld, A. Boukour, and Ch. Leclercq-Willain, Phys. Rev. C **48**, 468 (1993).
[4] G. R. Satchler and M. S. Hussein, Phys. Rev. C **49**, 3350 (1994).
[5] For an early application of the quantal particle flux to nuclear scattering, see I. E. McCarty, Nucl. Phys. **10**, 583 (1959).
[6] R. J. Glauber, in *Lectures in Theoretical Physics*, edited by W. E. Brittin and L. G. Dunham (Interscience, New York, 1959), Vol. I, p. 315.
[7] P. Roussel, N. Alamanos, F. Auger, J. Barrette, B. Berthier, B. Fernandez, L. Papineau, H. Doubre, and W. Mittig, Phys. Rev. Lett. **54**, 1779 (1985).